Chapter 15

BIOCERAMIC COMPOSITES

P. Ducheyne, M. Marcolongo, E. Schepers*
Department of Bioengineering, University of Pennsylvania, Philadelphia, USA
*Department of Prosthetic Dentistry, University of Leuven, Leuven, Belgium

INTRODUCTION

Man-made materials have been utilized for reconstructive and corrective procedures in the body for several centuries, but it was not until the late nineteenth century, when Lister described the principle of aseptic intervention, that any reasonable chance of success was possible. This was the first milestone on the way to our present day, highly sophisticated use of materials in the body. Through the twentieth century, until the late sixties, metals were the primary types of materials considered for implantation. The main impetus for use of ceramics in augmenting body tissues followed from Hulbert's work. Hulbert reasoned that metals, when implanted into the body, were not in their highest oxidation state, and would undergo ionization in the body. Depending upon the extent of ionization and the characteristics of the resultant dissolution product, there may be some degree of effect. Most ceramics are stable and do not ionize, and bioinert ceramics, such as alumina and carbon, are used as implant materials today and are described in Chapters 2 and 14.

It was not long before another class of ceramics was proposed for use in the body, the bioactive ceramics. It was argued that no material is truly inert, not only because of chemically induced reactions, but also from reactions due to the physical presence of the implant. It was proposed that an implant material would achieve highest compatibility if it allowed normal tissue at its surface.

The early development of bioceramics was prompted by considerations of biocompatibility, but implant devices must posses an appropriate range of mechanical properties. It was realized that for a number of biomedical applications, ceramics alone, either bioactive or inert, could not meet the diverse requirements of safe and effective *in vivo* functioning. This turned attention toward composite materials which could take advantage of the desirable properties of each of the constituent materials, while mitigating the more limited characteristics of each component.

Bioceramic composites can be divided in to three categories: bioinert, bioactive, and biodegradable composites. In these categories, the ceramic phase can be the reinforcing material, the matrix material, or both. Synthesizing a successful composite, follows identification of desirable properties as well as inferior characteristics of each material.

The desirable properties of bioceramics are:

inert:	minimal biological response, high wear resistance
bioactive:	enhanced bone tissue response, bone bonding
resorbable:	material is replaced by normal tissues, thereby excluding possible long term effects

However, these materials are limited for use in the body by:

inert:	limited mechanical properties in tension
bioactive:	limited tensile strength and fracture toughness
resorbable:	rate of strength reduction due to resorption may be too rapid.

There are several bioceramic composites which have been fabricated and analyzed (Table 1). These include stainless steel fiber/bioactive glass (the first bioceramic composite) and titanium fiber/bioactive glass composites. These discontinuous metal fiber/ceramic composites maintain bioactivity, while increasing the fracture toughness and strength of the material in comparison with that of the ceramic alone. There are also ceramic reinforced/ bioactive ceramic composites (e.g., zirconia reinforced/AW glass and apatite/wollastonite (AW) two phase bioactive glass ceramic), and bioceramic augmented polymeric matrices (e.g., calcium phosphate reinforced polyethylene). It has been shown that these composites are bioactive and have higher mechanical strength than the bioceramics themselves.

A look at bioceramic composite fabrication methods, mechanical properties, including fracture mechanics data as far as known, and *in vivo* reactions for static and dynamic load conditions will follow. The specific examples in this chapter are the stainless steel/bioactive glass and titanium fiber/bioactive glass-ceramic composites. However, it must be understood that the principles of composite design, fabrication, and analysis are applicable to many different bioceramic composites.

Table 1. Some Bioceramic Composites.

Inert	Carbon fiber reinforced carbon
	Carbon fiber polymetric matrix materials (polysulfone, poly aryl ether ketone, poly ether ketone ketone, poly ether ether ketone)
	Carbon fiber reinforced bone cement
Bioactive	A-W Glass-Ceramic
	Stainless steel fiber reinforced Bioglass®
	Titanium fiber reinforced bioactive glass
	Zirconia reinforced A-W glass-ceramic
	Calcium phosphate particle reinforced polyethylene
	Calcium phosphate fiber and particle reinforced bone cement
Resorbable	Calcium phosphate fiber reinforced polylactic acid

FABRICATION METHODS

Stainless steel fiber/bioactive glass composites are made of 45S5 bioactive glass and AISI 316L stainless steel fibers. The nominal composition for the bioactive glass is: 45wt% SiO_2, 24.5% CaO, 24.5% Na_2O, and P_2O_5. AISI 316L stainless steel has the following compositional range for the more important alloying elements: 16-20wt % Cr, 10-14 % Ni, 2-4 % Mo, less than 0.03 % C.

The preparation of the stainless steel fiber/bioactive glass composite involves a number of steps which includes preparing the fiber preform, impregnating the preform with the glass matrix, and heat treating the composite. Initially, the required amount of fiber for a given geometry is weighed and compacted under pressure, the fibers are sintered at 1250°C and then the uniformity of the preform's density is inspected using radiography. The surface of the sintered metal fiber preform is oxidized for 10 min in air at 800°C. The total metal shrinkage is controlled by holding the porous preform at 400°C for 20 min, and then it is immersed into molten glass maintained at 1350 to 1380°C, and finally the glass-impregnated preform is annealed at 400 to 500°C for 4 hours and furnace cooled. The processing parameters have been optimized experimentally to achieve this successful procedure.

For an effective stress transfer between the glass matrix and the reinforcing metal fibers, there must be a good bond between the glass and the metal fibers. This is achieved through the oxidation of the metal fibers before immersion in the molten glass. For a good glass to metal bond, the oxide layer on the metal itself must be adherent. Subsequently, this oxide layer must not dissolve completely in the glass during the immersion process. The enrichment of the main alloying elements in the inner layer of the formed oxide is responsible for the good adherence of the oxide on the metal. At the oxide-glass interface, the oxide is only partly dissolved. As a consequence, there is a graded transition from the glass to the metal fibers. Figure 1 illustrates this principle. There is diffusion of the iron in the glass, and there is also diffusion of the silicon into the oxide. This graded glass-metal interface corresponds to chemical adhesion of the constituents, so stress transfer from the glass matrix to the reinforcing metal fibers is much more effective than through a purely frictional interaction at the interface.

There are several variables which affect glass impregnation: viscosity of the molten glass, thermal expansion coefficients of the metal substrate and glass, oxidation and roughness of the metal surface, metal temperature at time of immersion, duration of immersion, time and temperature of annealing, volume fraction of the metal fibers and size of porosity.

Many of these variables were optimized through research in coating of metal rods with a glass layer, including viscosity, temperature and time of immersion. Of the remaining variables, the most significant challenges to the composite fabrication were thermal expansion of the metal and glass, and oxidation of the metal surface.

The mismatch between the thermal expansion coefficients of the glass and the metal fibers is significant. The values for stainless steel AISI 316L in 100μm fiber compact are 20.0 x 10^{-6}°C^{-1} (up to 200°C) and 21.8 x 10^{-6} °C (up to 400°C) and for bioactive glass 45S5 is 18.0 x 10^{-6} °C (up to 450°C). By combining the two materials,

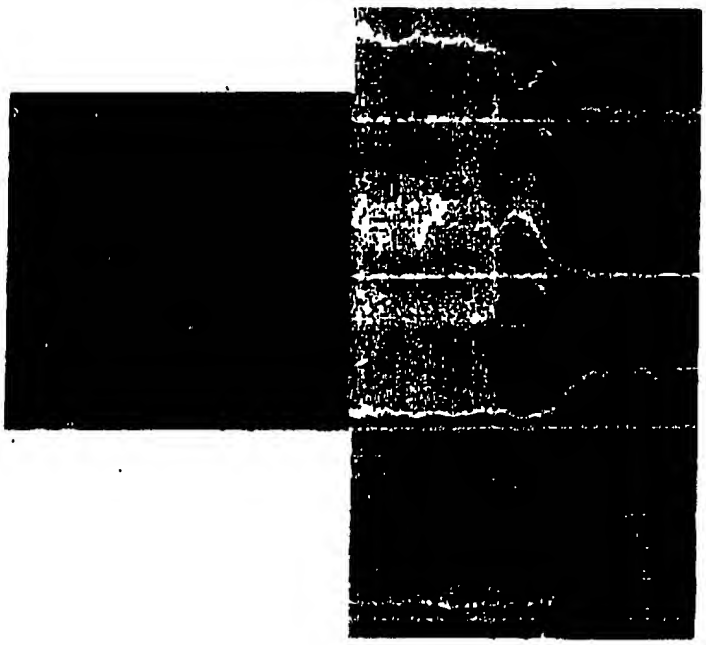

Fig. 1. Interfacial chemical analysis of the stainless steel fiber-to-glass-to-bone.

there is considerable potential for development of internal stresses during the cooling of the composite.

A variation on this general principle of impregnating a fiber preform can be found in the method used for fabricating a titanium fiber/bioactive glass composite. In using titanium, the difference in coefficients of thermal expansion is much greater. The thermal expansion coefficient of titanium is 8.7×10^{-6} $°C^{-1}$ in the 25 to 500°C temperature range. As a result it is impossible to reinforce bioactive glass 45S5 with titanium fibers. However, a titanium/bioactive glass composite is desirable since the titanium fiber, having excellent biocompatibility, would eliminate adverse tissue effects arising from the susceptibility of stainless steel fibers to crevice corrosion.

The bioactive glass used in the stainless steel fiber/bioactive glass composite is one of the most highly reactive bioceramics known. This is not always the best type of bioactive material for a composite because of the large reaction layer formed between the glass and bone, which leads to a weak interfacial strength. In designing the titanium fiber/bioactive glass composite, the glass composition was designed to have a slower bioactivity rate.

The fabrication process begins with the selection of the glass composition. 8-12% by weight Na_2O, 4-8% P_2O_5, 50-54% SiO_2, 0.5 -5% CaF_2 and the balance CaO leads to a bioactive glass-ceramic with a thermal expansion coefficient of $9 \times 10^{-6} °C^{-1}$ and a reaction layer about two orders of magnitude smaller than that of bioactive glass 45S5. The powder mix which will yield this composition, is melted, homogenized, and cast.

It is then cooled to obtain non-crystallized glass. The glass is annealed at 650°C for 4 hours, then ground finely to a mean particle size of 15 μm. The powder obtained has a homogeneous composition.

The titanium fibers, 4 mm long and 50 μm diameter, are pickled and cold compacted directly to the desired configuration. The titanium preform is placed in a copper or glass mold with the glass powder surrounding it, and vacuum closed. Hot isostatic pressing (HIP-ing) is carried out at a temperature in the range of 700 to 800°C at a maximum pressure of 1000 bars. This HIP-ing process results in glass impregnation of the titanium preform and partial crystallization of the glass, the extent of which depends of the HIP-ing cycle. Finishing includes polishing to ensure that the Ti-fibers are on the composite surface.

With this process, the surface distribution of the Ti is homogeneous, and the ratio of the area of visible fibers to the area of bioactive glass-ceramic is about 65:35.

MECHANICAL PROPERTIES

Tensile tests were done on a series of stainless steel/bioactive glass composites fabricated with 50, 100, and 200 μm diameter fibers, molded to different fiber volume fractions in the range of 0.4 to 0.6. The excess outer glass rim was removed by sand blasting and subsequent grinding on consecutive SiC paper on grits up to 320. Tensile test results are shown in Table 2, along with the properties of the parent glass and the porous fiber material. The results show that an increase in fiber volume percent of the 50 μm fibers caused a decrease of yield strength, while the ultimate strength remains unchanged; the modulus of elasticity also decreases. This observation apparently contradicts the theoretical assessment of the modulus of elasticity of composites, which

Table 2. Initial Tensile Tests of Stainless Steel Fiber/Bioglass® Composites.

Sample	Sample Type	$\sigma_{0.01}$(MPa)	SD	UTS (MPa)	S	E(GPa)	SD
50-S-45	Bioglass®-steel	59	5	80	17	112	13
50-S-60	composite	45	3	81	9	83	4
100-S-45		49	12	55	7	98	10
100-S-60		55	2	97	11	107	8
200-S-60		40	2	54	9	108	18
50-S-45	Porous fibre	20		70-110		35	
50-S-60	metal	42		140		65	
100-S-45		10		70		20	
100-S-60		30		135		65	
Bioglass® 45-S-5	Parent glass			42			

*Sample name is composed as follows; 1st figure represents the fiber diameter in μm, S represents stainless steel, and the second figure represents vol% of fibers.
®Registered trademark, University of Florida, Gainesville, Florida

projects a larger modulus for an increasing fraction of the higher modulus constituent (usually to a point of maximum stiffness, then any additional fibers cause a decrease in modulus, typically 60% is the maximum). In this case, the phenomenon may be caused by the fact that the distance between neighboring fibers has become too small to have a strengthening effect on the glass. In such a case, it is essentially the properties of the fiber phase of the composite which are measured. The compressive stress fields of neighboring fibers probably interfere with each other to such an extent that no appreciable strengthening can be achieved.

On the basis of these results, a second series of tensile and three-point bending tests were limited to composites made of either 45 vol% 50 μm (50-S-45) and 60 vol% 100 μm (60-S-100) fibers. Each of these specimen types had three different surface finishes, with final grinding grits of 80, 320, and 600. The results of this second series of tensile and bending testing are compiled in Table 3. Figure 2 shows a series of specimens after testing: this figure clearly documents the extensive plasticity that can be achieved by modifying bioactive glass into a glass-metal fiber composite. The surface finish had no appreciable effect on the mechanical properties of the different samples, and so the data can be considered *en masse*. Both the bending and tensile strengths of the composites are significantly higher than those of the parent glass or the fiber mesh. There seems to be little difference in the mechanical properties of the 50-S-45 and the 100-S-60 composites.

Table 3. Mean Strength Values of Two Stainless Steel Fiber/Bioglass® Composites, as Measured by Tensile and 3-point Bending Tests.

Sample	Mode of Testing	σ0.01(MPa)	SD	$\sigma_{0.2}$(MPa)	SD	UTS(MPa)
50-S-45	Tension*	60.9	11.8	78.3	11.2	91.9
	Bending†	----		167.6	38.4	290.4
100-S-60	Tension*	57.0	8.6	73.3	7.1	97.9
	Bending†	----		162.9	31.4	339.9

*Twenty specimens
†Ten specimens

The strength values of the composites are close to the upper bound value which can be assumed by

$$\sigma_c = \sigma_{uf}\nu_f + \sigma_{um}\nu_m \quad (1)$$

where σ_c is the composite strength, σ_{uf} is the ultimate fiber strength, ν_f is the fiber volume fraction, and ν_{um} is the matrix volume fraction. This equation is valid within the assumptions of continuous reinforcement of aligned fibers, equal strains in both components and absence of internal stresses. With a σ_{uf}=530MPa and σ_{um}=42MPa, the composite strengths given in Table 4 are obtained. However, since internal compressive stresses are present in the glass fraction, and since the matrix stress, σ_{um}, is probably larger as the glass is strained as small volumetric units, the strength by just combining

Fig. 2. Series of mechanically tested specimens: notice the extensive deformability of this glass-metal composite.

Table 4. Calculated and Measured Strengths of Two Optimized Microstructures of Stainless Steel Fiber/Bioglass® Composites.

	Composite Strength (MPa)	
Composite	Calculated	Measured
50-S-45	262	290
100-S-60	335	335

These calculated values are very close to the measured values.

two materials should be lower than the calculated numbers. There is still room for increasing the strength of this particular fiber reinforced glass composite, probably by full optimization of the fiber diameter, the respective volume fraction of each constituent and the fiber/glass bonding.

In another series of tests, the four point bend fracture strengths were measured as a function of strain rates. These tests were performed on the 50-S-45 and 100S-60 composites. As seen in Fig. 3, there is a linear relationship between the logarithms of fracture strength and strain rate, which indicates that the properties of the composite are still markedly dependent on the properties of the ceramic phase, since fracture mechanics theory of ceramics, unlike the theory for metals, prescribes this linear relationship.

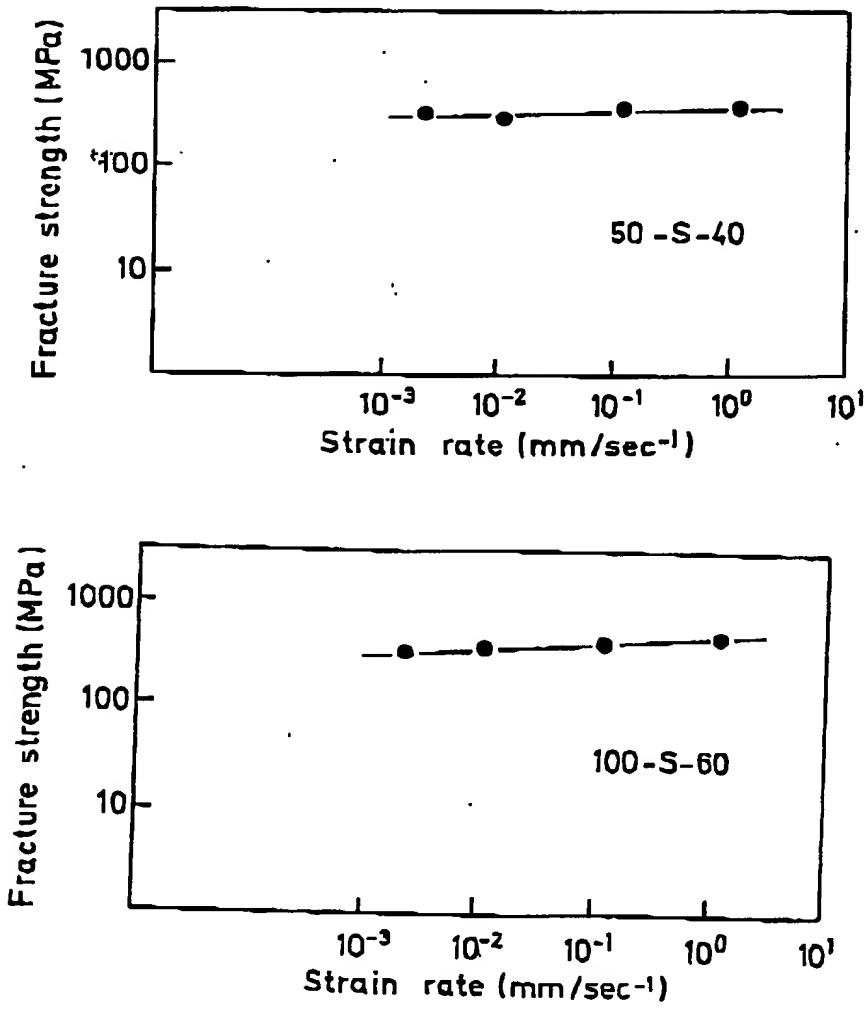

Fig. 3. Fracture strength as a function of strain rate for two stainless steel fiber/Bioglass® composites.

There is a marked difference in fracture between the two types of composites is bent heavily with local cracks at the surface. A fractographic analysis demonstrates the significance of these results.

DUCTILITY AND FRACTOGRAPHIC ANALYSIS

The stainless steel-bioactive glass composites display a marked ductility. In tension testing, up to 10% deformation to failure is observed. In three-point bend testing plastic deformation until a bend angle of over 90 degrees is invariably obtained; this was the maximum attainable with the experimental set-up used.

The onset of plastic deformation of the composite is probably caused by plastic deformation of the metal fibers. Subsequently, multiple cracking of the matrix occurs. Fractographic analysis shows cracks in the glass, perpendicular to the tensile direction, with blunting of the cracks by fibers. Cracking is extensive at the fracture surface, but is limited away from it. There is no debonding between fiber and glass except at the fracture surface and its immediate vicinity. This indicates that stress transfer between fiber and glass remains good until structural damage is close to yielding complete failure of the composite. Only then does debonding and fiber pull-out take place.

Scanning electron microscopical (SEM) examination reveals that the extensive elongation at the fracture surface is almost solely due to the stretching and pull-out of the fibers from the glass matrix; there is little glass between the fibers and it is the fibers that are torn and not their sinter-bonds. Figure 4 are SEM micrographs of this finding. After debonding between glass and fiber occurred, the stretched fibers elongated without the glass. Only at spots where the cracking was perpendicular to the fiber does the glass remain on the fiber.

The reinforcement of the glass caused by the fibers is threefold:

1. *The cohibitive effect:* if the bond between the fibers and the glass is good, stress transfer between both is effective. The main portion of the stress then acts upon the constituent with the greatest modulus of elasticity, in the present case, the metal fibers. As the stress in the glass matrix is decreased, subcritical crack growth is hindered.

2. *The cooperative effect:* if cracks grow in the glass matrix, they are blunted by the presence of the fibers. The stress concentration at the tip of the crack is reduced initially by the plastic deformation of the fibers. A subsequent mechanism which can be operative when substantial gross deformation has occurred, is the decohesion between the glass and fibers, followed by pull-out of the fibers.

For both effects, the cohibitive and cooperative effect, the glass-to-metal interface plays an important role. There must be a compromise between the contradictory requirements for strength and toughness. Best strength is reached for a high interfacial bond between the glass and the fibers, but the fiber pull-out which adds considerably to toughness, requires decohesion between the glass matrix and the metal fibers. In the present composite, initially good interfacial bonding is achieved for high strength, and fiber pull-out occurs with substantial gross deformation of the fibers.

3. Crack initiation and propagation is also hindered by residual compressive stresses in the glass matrix. This is due to the difference in thermal expansion between fibers and glass, which puts the glass in compression. Here also, a good interfacial bond is essential to carry the induced stresses at the glass/metal interface.

TISSUE RESPONSE

Static Load Conditions

In view of potential clinical applications of bioactive glass composites the biological tissue response must be evaluated, examining the difference in material's and host's tissue response to bulk glass and bioactive glass metal composites, the effect of

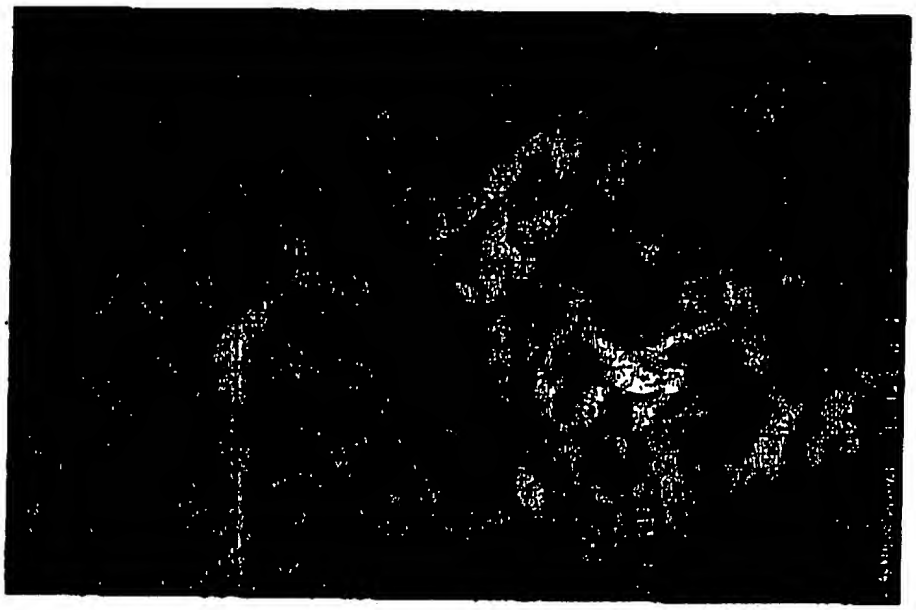

(a) Overview of the fracture surface (fiber diameter: 50μm).

(b) Fiber pull-out and fiber-rupture.

Fig. 4. Scanning electron micrographs documenting some of the reinforcement mechanism of the metal fiber-bioactive glass composites.

Fig. 4. Continued.

(c) Oxide scale spalling off at ultimate failure indicating excellent adhesion between matrix and fiber.

(d) Glass remnant in the center of the photograph, indicating continuous matrix-to-fiber stress transfer till final fracture.

a possible exposure of the metal fibers, the subsequent interaction of released metal and glass ions, the influence of time on the interfacial reactions and the thickness of the reacted glass layers.

Implantation experiments were first done under static load conditions to evaluate the bonding behavior of the stainless steel/bioactive glass composite. Bioactive glass composite plugs with a diameter of 5mm and a length of 8mm were implanted for 8 weeks in the femora and tibiae of dogs, together with control bulk bioactive glass and control bulk stainless steel specimens. The specimens were implanted under statically loaded conditions. The shear strength of the bond-plug was measured by a push-out test.

The results of the push-out test are presented in Fig. 5. Stainless steel specimens were encapsulated by fibrous tissue. The plugs required only minimal force to be pushed out of the capsule. In contrast, the bioactive glass and the bioactive glass composite plugs bonded to bone. Comparing the measured shear strengths with respect to position of each plug and thus the intrinsic strength of the surrounding bone, the experiments do not show a significant bonding difference between bioactive glass and bioactive glass composites.

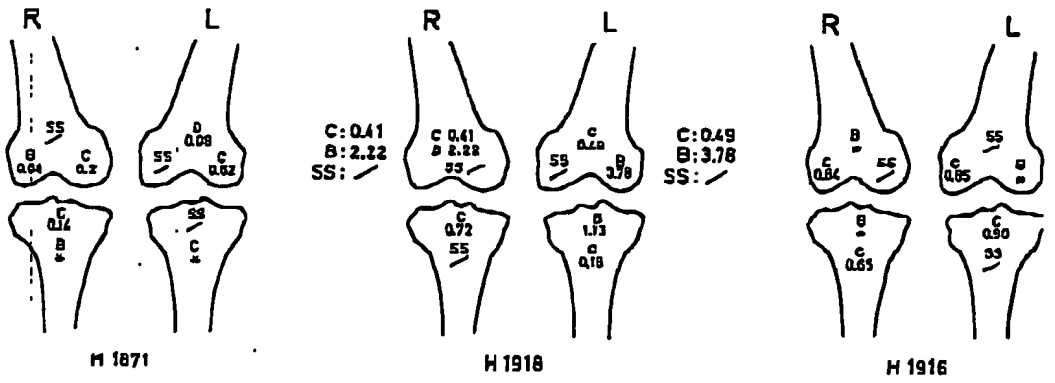

Fig. 5. Mechanical test results of stainless steel fiber/bioactive glass composite push-out testing. Shear stress units are in MPa. C represents composite, B for bioactive glass, SS for stainless steel. An asterisk means that the bone surrounding the specimen was damaged inadvertently during dissection. (From Gheysen et al. *Biomaterials*, V4, (1983) with permission.)

Stainless Steel Fiber Reinforced Bioactive Glass as Tooth Root Implant

Beagle dogs were used as experimental animals in a dental root implant study. The premolars were extracted at least one year prior to implantation. With appropriate anesthesia cavities were prepared in the edentulous areas. Low-speed drills (approximately 300 RPM) with abundant cooling by physiological saline were used for all the preparations. Three dogs received subgingivally six fiber-reinforced bioactive glass implants with a pin of bioactive glass on the surface and one bulk bioactive glass, as a control. They were killed 4 months after implantation. In one animal five bulk bioactive glass implants were installed in the lower jaw and two in the upper jaw. This animal was killed after 16 months.

Following the usual preparation for light and SEM no difference in the reaction pattern between bulk bioactive glass and fiber reinforced composite glass was observed at 4 months (Fig. 6). The various reaction layers present on the composite glass were similar to those reported previously. Energy dispersive X-ray (EDX) analysis clearly demonstrated the formation of a Si-rich layer covered by a CaP-rich layer at the outer surface.

Fig. 6. Micrograph of the interfacial zone between stainless steel-bioactive glass composite and bone tissue.

Histologically, connection between the implant surface and bone is readily apparent: it is preferentially present at the cortical bone border. No interposed fibrous tissue can be seen between the implant and the bone. The osteocytes at the interface are regularly distributed and some cell processes in the canaliculi of these cells appear to be in a very close relationship with the reacted implant surface. EDX analysis of the Ca-P rich layer in such an interface shows an increasing Ca and P concentration at the outer glass surface and a smooth transition of the Ca and P peak intensities towards the bone tissue. This results in a compositional gradient between bioactive glass and bone tissue. In contrast, when the implant is surrounded by fibrous tissue the Ca and P profiles increase toward the outer surface but drop immediately to zero when the neighboring tissue is scanned. This fibrous encapsulation of the implant is preferentially seen at the apical part of the implant, near the infra-alveolar nerve where no bone tissue is present at the time of installation. The fibrous tissue capsule consists of dense packed collagen fibers and contains few cells. These observations confirm that bioactive glass is not osteoinductive since bone connection is only formed when bone tissue is present in the immediately vicinity of the glass surface at the time of installation. This lack of osteoinductivity also is substantiated by the absence of bone tissue at the glass surface

around a perforation to the maxillary sinus. Close adaptation of the epithelial tissue to the glass surface is observed here. Whereas no osteoinduction can be ascribed to the glass, it is osteoconductive. An outgrowth of bone can be observed in the apical and the cervical directions, where it starts from the initial contact area with cortical bone.

When the implant is intact, EDX analysis does not reveal any ion diffusion from the metal fibers into the outer glass rim of the implant or in the surrounding tissues. Thus, the outer glass rim is effective in preserving the biocompatibility of the bioactive glass itself, and prevents any influence of the stainless steel fiber. However, if metal fibers are directly exposed to the surrounding tissue fluids, Fe ions from the stainless steel fibers are detected by EDX point analysis in tissues of these areas. Other metal ions are not detected, but this can be due to the detection limit of this technique (approximately 0.01 - 0.1%). These metal ions inhibit the interfacial osteogenesis in these areas and can even elicit an inflammatory cell reaction. Since these reactions are not consistently observed, it is suggested that the tissue response in areas with a cracked glass rim is due to the synergistic action of dissolved glass ions and metal fiber ions.

Stainless Steel Fiber Reinforced Bioactive Glass Dental Implants Under Dynamic Load Conditions

The mechanical properties of the bioactive glass are substantially improved by reinforcing the glass with stainless steel fibers and it may appear that a structurally reliable material is available. However, one still must consider the strength of the reacted glass layer at the outer surface. The bonding of the bioactive glass to bone tissue is associated with a series of chemical reactions, resulting is a Si-rich layer on top of which a CaP-rich layer is formed. The Si-rich layer is a hydrated silica gel, with low mechanical properties. In a study in which chewing forces acted on the stainless steel fiber-reinforced bioactive glass implants with an outer rim of pure glass, it was shown that even in the presence of an established glass-bone bond, this reaction zone is susceptible to shearing upon loading. Upon a topical shear failure of the reacted glass layer, the glass leaching reactions are perpetuated and eventually the underlying metal fibers are exposed. Since it has already been shown that the stainless steel fibers must remain covered by a rim of glass, the exposure to the surrounding tissue fluids of the stainless steel fibers is the last step in the failure of stainless steel-glass composites to achieve long term bonding under functional load conditions.

Titanium Fiber Reinforced Bioactive Glass Ceramic Dental Implants under Dynamic Load Conditions

The outcome of clinical studies with stainless steel/45S5 composites is drastically altered by modifying the composite in two ways, replacing stainless steel by titanium, and modifying the bioactive glass to be less reactive. A study aimed at determining the integrity of the bond under functional load conditions for time periods of up to two years is nearly completed.

Implants were installed in the partial edentulous lower jaws of beagle dogs, four in each half. After three months of subgingival installation of the "root" parts of the

implants, the permucosal parts were connected. On top of the implants, fixed crowns or bridges were installed. This resulted in the application of chewing forces to the bone-glass composite interface. Clinically these implants have been functioning very well during the experimental period. This must be contrasted to the glass-stainless steel fiber implants which all failed clinically within two weeks of transmittal of occlusal forces.

The formulation of this new composite, comprising titanium fibers and bioactive glass-ceramic, both intentionally exposed at the surface, was based on two animal studies. One of these studies illustrates that bioceramic composite development can be based on a fundamental understanding of the properties to be achieved.

Tissue Response to a Bioactive Glass-metal Interface

In order to study whether the exposure of any metal in contact with glass to surrounding tissues is precluded, a comparative analysis of bioactive glass in contact with titanium, wrought Co-Cr alloy and stainless steel was done. A series of 24 implants was installed in the femora and tibia of two beagle dogs and resected after 3 months. These implants were made from a bioactive glass cylinder jacket and a cylindrical bolt and nut with the same diameter as the glass jacket and made of either stainless steel AISI 316L, commercial pure titanium, or wrought Co-Cr alloy.

In this study bioactive cylinders showed an intensive bone bonding and osteoconductivity, resulting in a complete bony encapsulation of the glass. The metal bolts and nuts showed a direct contact with bone tissue, but only in areas of presumed bone contact at the time of implantation. Osteoconduction was not seen on these metal surfaces. The extent of bone contact decreased from titanium to wrought Co-Cr alloy to stainless steel.

Osteogenesis was frequently disturbed at the stainless steel or cobalt chromium to glass interface, shown by a focal absence of bone formation in this area. This ring-shaped non-calcified tissue contained non-inflammatory cells. Occasionally inflammatory cells like macrophages and histiocytes were seen but only with stainless steel which evoked a much more pronounced reaction than the Co-Cr alloy, which in its turn was more intensely reactive than titanium. In the case of titanium, bone formation did not appear to be hindered. When small crevices occurred between the bioactive glass cylinder jackets and the metal bolts or nuts, the superiority of titanium was evident. These crevices were mostly invaded by fibrous tissue, except for titanium where bone grew into the entire crevice (Fig. 7).

The results of this study together with findings on reduced glass reactivity prompted the synthesis of the titanium-glass ceramic composite which currently has undergone extensive evaluation under non-functional load conditions. Once histological evidence of bonding under long term functional load conditions is seen, human clinical trials can begin.

The experiments showed that bone bonding is established at the bioactive glass islands in between the titanium fibers at the implant surface. Bone tissue jumps from one bioactive glass island to another, and, with only a small titanium fiber separating the glass, close bone apposition to this titanium surface is achieved. Figure 8 shows bone

Fig. 7. This back-scattered image shows the good penetration of the glass between the sintered stainless-steel fibers and the good wettability of the metal fibers. The reacted glass layer is bonded to the bone tissue. BG = unreacted bioactive glass, RG = reacted glass layer, B = bone, F = metal fiber.

Fig. 8. Bone grows (arrows) into the crevice between the bioactive glass and the metal, adheres to the glass surfaces and contacts the titanium surface. Oxidized titanium sample. B = bone, BG = bioactive glass, M = metal. Giemsa stain, original magnification X100.

tissue in direct contact with the glass ceramic-titanium composite. The optimal distribution ratio of titanium fibers and glass varies between 60/40 and 70/30. The glass islands are slightly dissolved after three months of implantation. This creates undercut areas at the implant surface by which the initial exclusively chemical bonding of the implant in the jawbone is enhanced by mechanical interlock.

CONCLUSION

Bioceramic composite synthesis serves the purpose of enhancing mechanical behavior of the parent ceramic, while maintaining its excellent biocompatibility and, if applicable, bioactivity. The approach of reinforcing bioactive glass with metal fibers imparts to the bioactive glass an unusual fracture toughness. If the fiber selected is titanium, this fiber can be exposed to body fluids and a well-bonding glass composite is obtained.

The titanium fiber bioactive glass composite represents a fundamental advance in biomaterials, which derives from consideration of the failure mode of current implants with bioactive coatings as bonding vehicles. Dental implants or hip prostheses with plasma sprayed calcium phosphate coatings are known to fail at the ceramic to metal interface. The advent of the titanium fiber-glass composite represents a new era in that a continuity between metal implant and bioactive coating may be achieved, using fibers that are sintered onto the implant substrate and then run throughout the coating up the surface.

READING LIST

P. Ducheyne, and L. L. Hench, "The Processing and Static Mechanical Properties and Metal Fibre Reinforced Bioglass®," *J. Materials Science* 17 (1982) 595-606.

A. Evans, *Fracture in Ceramic Materials* (Noyes Publications, Park Ridge, NJ, 1984).

E. Schepers, M. De Clercq and P. Ducheyne, "Tissue Response to a Bioactive Glass-metal Interface," in *Implant Materials in Biofunction. Advances in Biomaterials, Volume 8*, ed. C. de Putter, G. de Lange, K. de Groot, and A. Lee (Elsevier Science Publishers B.V., Amsterdam, 1988) pp. 79-85.

S. Tsai, and H. Hahn in *Introduction to Composite Materials* (Technomic Publishing Co, Inc., Lancaster, PA, 1980).